



DIRECTIONAL ACOUSTIC ATTENUATION OF PLANAR FOAM RUBBER WINDSCREENS FOR PHASED ARRAYS

Robert P. Dougherty^{1,2}

¹OptiNav, Inc.

1414 127th PL NE #106, Bellevue, WA, 98005, USA

²University of Washington, Aeronautics and Astronautics Department
Seattle, WA, 98195, USA

ABSTRACT

Use of a porous layer, such as foam rubber, over a phased array is proposed to reduce background noise in wind tunnel acoustic measurements. As previous work has shown, this reduces boundary layer noise by displacing the flow from the array by the thickness of the layer. The new idea is that it can also reduce the impact of noise from the wind tunnel drive system and other flow control features because that noise appears to originate from far away in the wind tunnel, usually upstream. Due to its oblique incidence on the porous layer, the interfering noise sees more transmission loss in passing through the layer than the sound from the model does. A disadvantage of such a layer is that the attenuation can increase rapidly with frequency, possibly complicating the interpretation of the data. Shop tests of several materials have been performed. It is observed that viscoelastic “memory foam” has lower and more-linear attenuation than the other samples tested. Elements of the shop results have been validated in a wind tunnel test.

1 INTRODUCTION

Many aeroacoustic measurements are best done in wind tunnels, and acoustic wind tunnels are not common. If the model is loud enough and the frequency is reasonably high, then a phased array should be able to measure the intended sound. Some models are designed to be quiet, and the wind tunnel may not be quiet at all, so the array may not have sufficient dynamic range for the job. Approaches that have been suggested include applying wave number analysis to decompose the array cross spectral matrix (CSM) [1] and subtracting empty tunnel noise from the CSM [2]. These measures themselves have limited dynamic range, and more noise suppression may be needed. Another noise source in a closed wind tunnel is boundary layer turbulence. This is often treated by deleting the diagonal elements of the CSM [3] and/or recessing the array below a Kevlar screen [4], [5]. An acoustic foam layer covered by a perforated metal plate has also been used [6].

2 CONCEPT

2.1 Arrangement

The idea is illustrated in Fig. 1. The wind tunnel test section is shown. The arrows represent sound rays propagating through the foam layer (shaded). The noise from the model is more or less normally incident on the array, and takes a short path through the absorbing material. The background noise should have more transmission loss due to the longer path length through the material. A speaker measurement would be used to calibrate the model transmission loss as a function of frequency and possibly angle so that the data can be corrected for this loss. The porous layer is shown outside the wind tunnel wall, which would be a simple installation but may alter the flow. An alternative would be to recess the array so that the surface of the layer conforms with the wind tunnel wall.

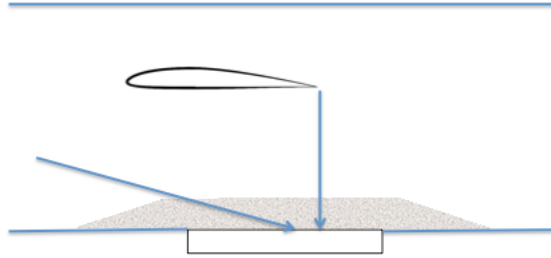


Fig. 1. Arrangement of the porous layer in a wind tunnel. The microphone array is at the bottom. Background noise travels through more of the layer than noise from the model does.

2.2 Analysis

For a single frequency, ω , suppose the characteristic impedance of the porous material normalized by the characteristic impedance of air is denoted W_r . Similarly, let $k_0 = \frac{\omega}{c}$, where c is the speed of sound in air, and write $k_r = \frac{k}{k_0}$, where k is the wave number in the porous medium. In studies of acoustic propagation in porous media, both W_r and k_r are considered to be complex functions of frequency [7-9]. Suppose a plane wave is incident on the foam layer attached to the array surface with angle of incidence θ , as shown in Fig. 2. Enforcing continuity of the acoustic pressure and velocity at the air-foam interface and zero normal velocity at the array gives

$$\left| \frac{p_{\text{array}}}{p_{\text{no foam}}} \right|^2 = \frac{1}{\left| \cos(kh) + j \frac{\sqrt{1 - \left(\frac{\sin\theta}{k_r}\right)^2}}{W_r \cos\theta} \sin(kh) \right|^2} \quad (1)$$

Among the many models for the acoustic properties of porous media, the simplest and best known is the Delany and Bazley model [9-12]. In this model, the flow resistivity, R_1 , is combined with the density of the air inside the porous medium, ρ , and the frequency, $f = \frac{\omega}{2\pi}$, to form the dimensionless parameter

$$X = \frac{\rho f}{R_1}. \quad (2)$$

The acoustic quantities are then modelled according to

$$W_r = 1 + c_1 X^{c_2} + j c_3 X^{c_4} \quad (3)$$

$$k_r = 1 + c_7 X^{c_8} - j c_5 X^{c_6} \quad (4)$$

where $c_1 = .0571$, $c_2 = -.754$, $c_3 = -.087$, $c_4 = -.732$, $c_5 = .189$, $c_6 = -.595$, $c_7 = .0978$, and $c_8 = -.7$.

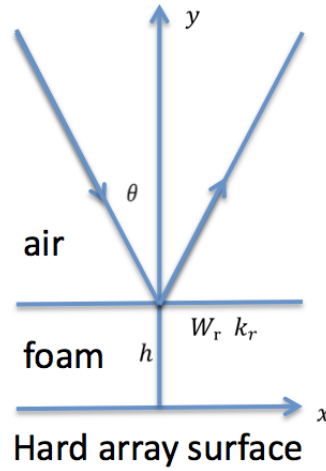


Fig. 2. Parameters for analysis.

2.3 Flow resistivity measurements

The rig shown in Fig. 3 was constructed to measure flow resistivity of foam samples. The blower supplies air to the right end of the pipe, which contains straws for flow conditioning. The sample is mounted inside between pressure taps 1 and 2, supported by a wire screen. The pressure difference $p_2 - p_3$ across the nozzle is used to determine the mass flow, m . The flow resistivity in MKS rays/m is then computed by [11]

$$R_1 = \frac{1.18(p_1 - p_2)A}{ml} \quad (5)$$

where A is the area and l is the thickness of the sample.

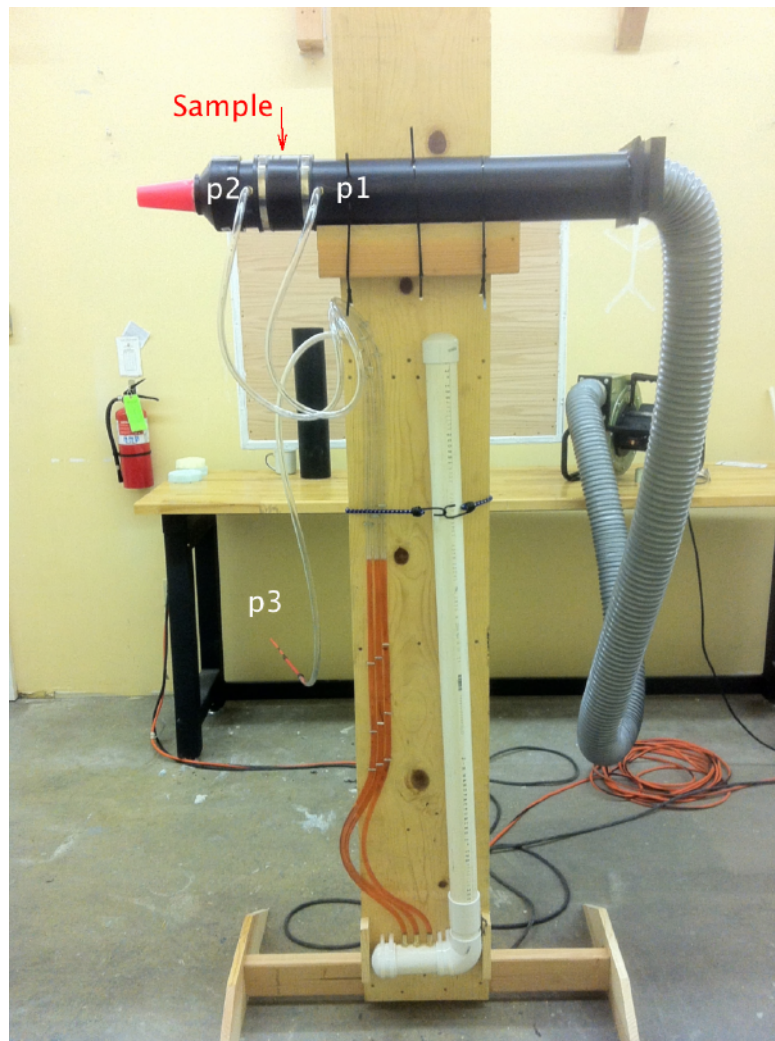


Fig. 2. Flow resistivity rig.

2.4 Test setup for characterizing layers

A speaker was positioned in relation to a phased array as shown in Fig. 2. A layer of foam is positioned in front of the array. The speaker is located at the 60° angle in the figure; it was also tested at 0° (normal incidence) and 80° (near grazing), using a polar distance of 2 m from the center of the array in each case.

The insertion loss was measured by broadcasting white noise with the speaker and measuring array data with and without the foam in place. Conventional frequency-domain beamforming was applied and the peak level for each band was used to compute the transmission loss.



Fig. 3. Setup for insertion loss testing. A 0.7 m aperture phased array is shown, but a smaller array, Array 24 Jr. (0.35 m) was actually used for the measurements.

2.5 Foam materials

Five samples of polyurethane foam were studied. Images of the foam surfaces are shown Fig. 4 and properties are given in Table 1. The column labelled IFD in Table 1 is a manufacturer's specification of stiffness. The resistivity values shown in Table 1 were measured using the rig pictured in Fig. 2. Memory foam is a viscoelastic material that springs back to its original shape slowly after being compressed and released. The viscoelastic properties depend on temperature. The measurements reported here were conducted at about

15° C. The term "acoustic foam" for sample 5 appears to be a marketing designation. It is stiffer and less dense than the other samples.

Table 1. Properties of Polyurethane Foam Samples Tested

No.	Type designation	Nominal density, lbs/ft ³	IFD	h, cm	h, in.	Measured Density, kg/m ³	R ₁ , MKS rayls/m
1	2040	2.0	40	2.54	1	34.5	30000
2	41b memory foam	4.1		2.54	1	60.8	24000
3	1833	1.8	33	5.08	2	31.2	35000
4	41b memory form	4.1		5.08	2	60.8	20000
5	P170-80 acoustic foam	1.7	80	5.08	2	23.3	27000

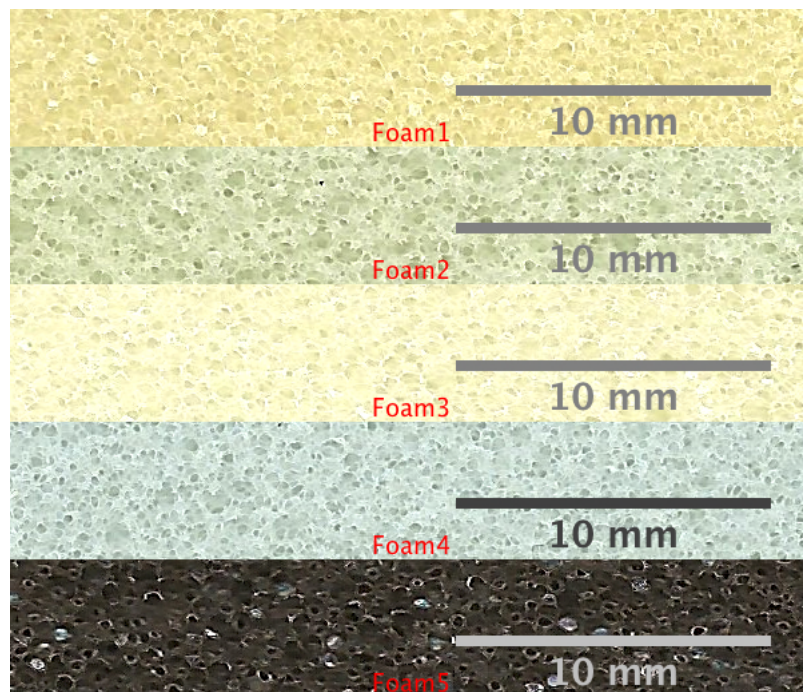


Fig. 4. Foam material samples.

3 FOAM RESULTS

3.1 Sample beamform plots

Typical beamforming results are shown in Fig 5, which gives plots for no treatment, a), and the memory foam, b). The loudest spot represents direct propagation in each case. The second loudest spot is a reflection in the floor. By choosing the highest level in the map, reflections and sidelobes are disregarded. Deconvolution processing and integration were not applied in this case, because the speaker is regarded as a point source, and its observed level is all that is needed. In the case of Fig. 5, the speaker level is 84.78 dB with no treatment and 74.35 dB with the memory foam, so the material has a transmission loss of 10.43 dB at 60° in the 6,300 Hz 1/3 octave band. Note that the focusing distance was set to 0.94 m. This distance

was found by performing a z-sweep to search for the highest level, and is approximately 2 m times $\sin 60^\circ$.

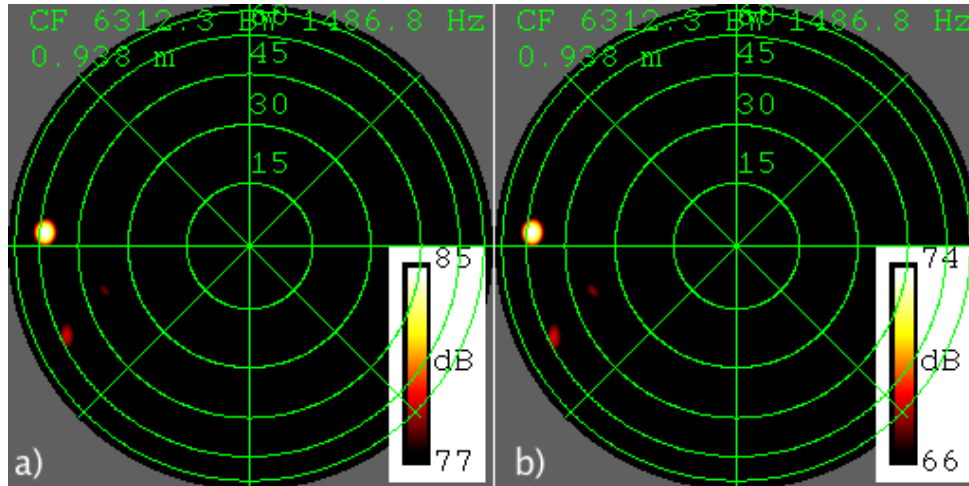


Fig.5. Representative beamform maps for the 60° angle. a) no treatment, b) memory foam.

3.2 Transmission loss spectra

Figs. 6 & 7 give the 1/3 OB insertion loss spectra for samples 1 and 2, respectively, at 0°, 60°, and 80°. There is no apparent insertion loss at frequencies of 1 kHz and below. For higher frequencies, the insertion loss is quite significant, and increases with the angle of incidence. Comparing Figs. 6 and 7, it is seen that the memory foam (sample 2) has lower insertion loss at normal incidence and about the same insertion loss at 80°, compared with the ordinary foam. This suggests that sample 2 would be more useful for this application than sample 1 would be. Figure 8 gives the insertion loss for the two samples at 60° and 80° relative to the insertion loss at 0°. At high frequency, sample 2 has less relative insertion loss at 60° than sample 1, and, again, more relative insertion loss at 80°. This is probably desirable from the point of view of using sample 2, since the 60° angle is likely to be more associated with model noise than wind tunnel background noise.

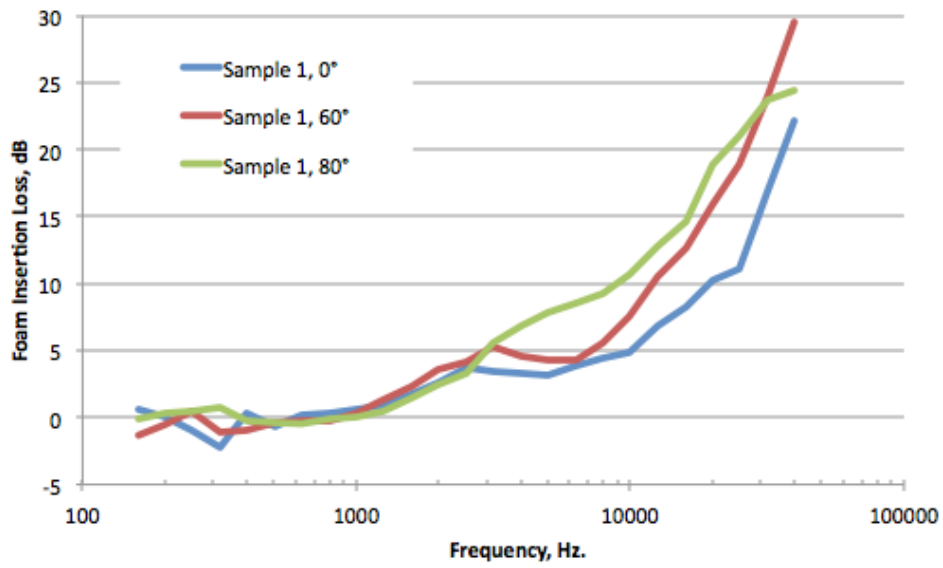


Fig.6. Insertion loss for three angles of incidence for sample 1.

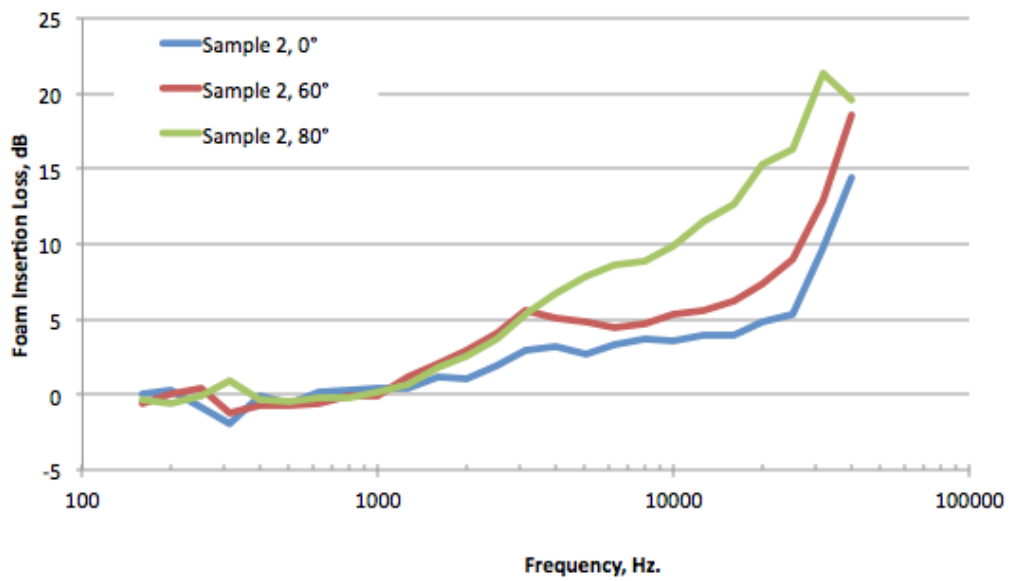


Fig.7. Insertion loss for three angles of incidence for sample 2.

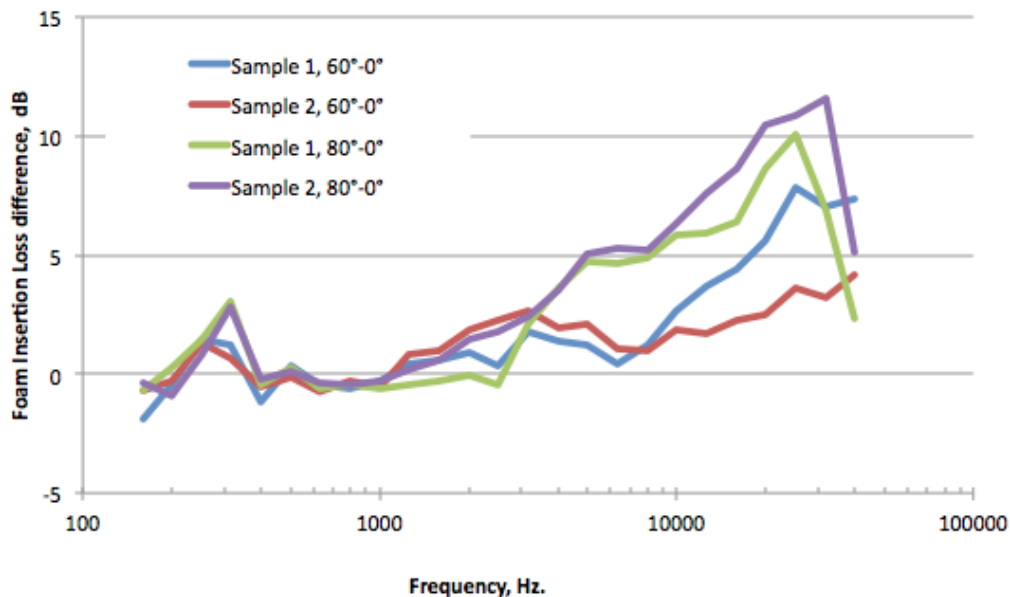


Fig.8. Excess insertion loss at 60° and 80° compared with normal incidence for samples 1 and 2.

Results from the thicker samples are given in Figs. 9-11. In Fig. 9, the normal incidence insertion loss is compared with the result of applying the Delany and Bazley model in Eq. 1. The model and the data agree about the order of the results: higher resistivity gives higher insertion loss. At high frequency, the normal incidence agreement is reasonable for the conventional foams, samples 3 and 5, but the memory foam is strikingly lower than the other samples and the model. Sample 1 has so much normal incidence insertion loss at high frequency, 40-50 dB above 20 kHz, that it may not be feasible to compensate for it in processing. This suggests that 5 cm is too thick for the conventional foam. The memory foam, in contrast, may be acceptable at this thickness.

At 80° (Fig. 10), the insertion loss predicted by the model increases across the frequency range, but this increase is not observed in the data at low frequency (1000 Hz and below). It is possible that a flanking path problem is reducing the observed insertion loss at low frequency. Deconvolution processing may have improved the results.

The selectivity of the 5 cm memory foam for rejecting interference at 80° is shown in Fig. 11. More than 15 dB is seen in the data at high frequency, but the model does not predict it. In contrast, the model shows more selectivity than the data at low frequency.

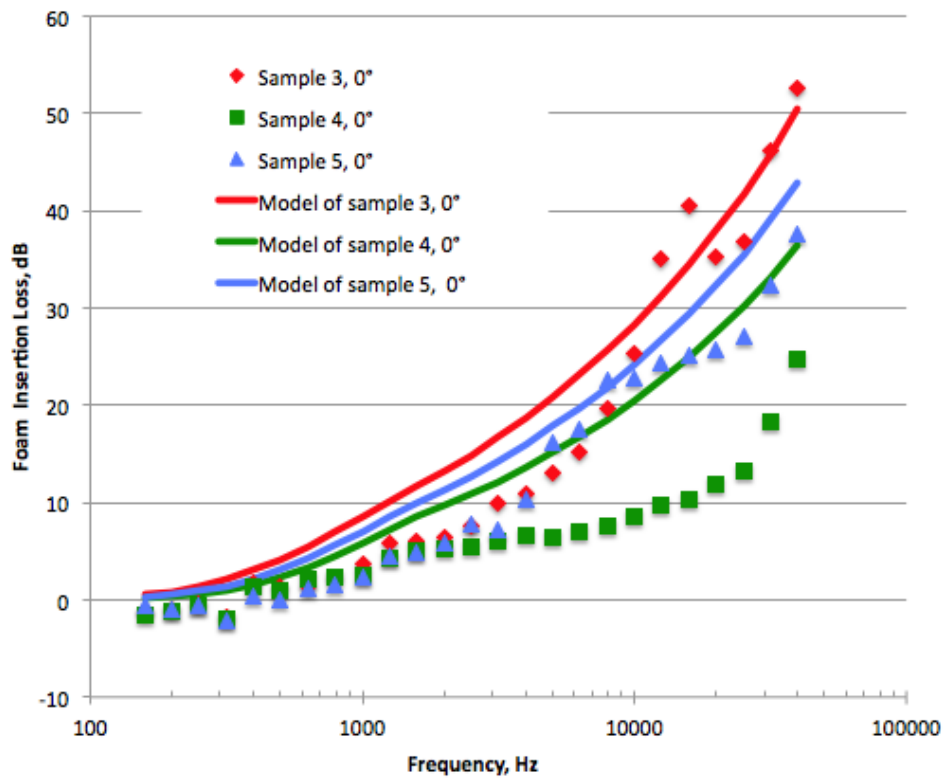


Fig.9. Normal incidence insertion loss for samples 3-5: measured and Delany and Bazley model .

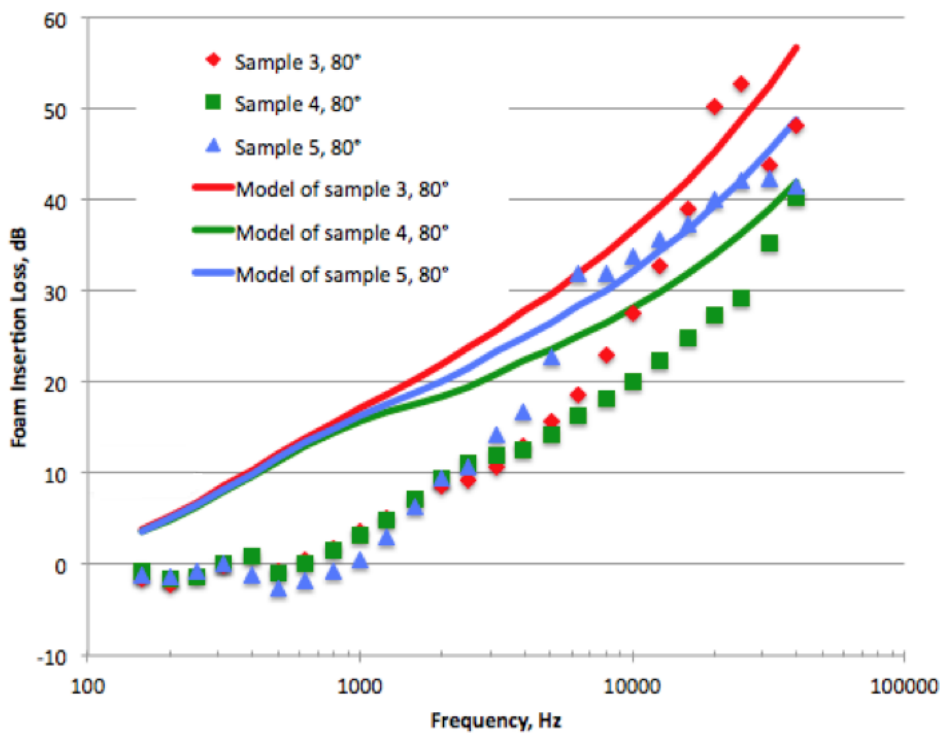


Fig.10. 80° incidence insertion loss for samples 3-5: measured and Delany and Bazley model.

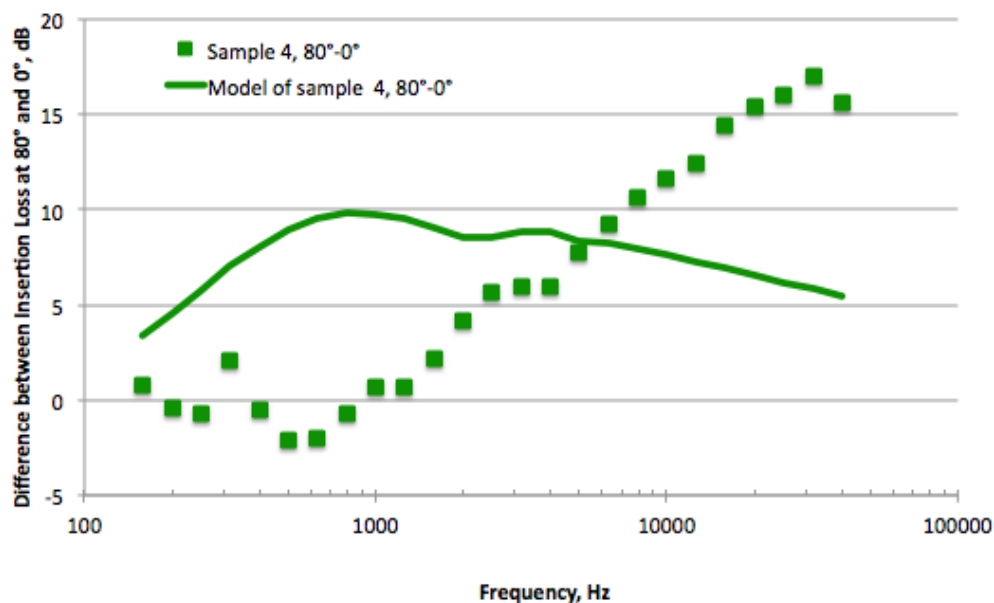


Fig.11. Difference between 80° and 0° insertion loss for sample 4: measured and Delany and Bazley model.

3.3 Wind tunnel test

The effect of foam (sample type 1) in an actual wind tunnel test was evaluated in the Kirsten Wind Tunnel at the University of Washington. An array of 8 G.R.A.S. microphones in a wooden housing was installed on the floor of the test section under a partially assembled model, as shown in Fig. 12. Data were acquired at a speed of 40 m/s with no foam and with a sheet of foam installed as shown in Fig. 13. (The wind tunnel speed was selected because the foam fluttered at 50 m/s. Fig. 12 should not be taken as an appropriate installation technique for foam in wind tunnel.)

The insertion loss spectrum for the foam is shown in Fig. 13. The noise metric for the plot is the reduction in the average of the off-diagonal elements of the Cross Spectral Matrix. This quantity was selected because the off diagonal elements should be less sensitive to the effect of the turbulent boundary layer than the microphone auto spectra would be, and the foam reduces boundary layer noise as well as reducing acoustically propagating noise. This measure may not be completely successful in this case because a dynamic test method (e-stop!) was employed and this reduced the integration time for each speed to about one second. Over most of the frequency range between 1000 and 20,000 Hz, the insertion loss in Fig. 13 is comparable to the 80° curve in Fig. 6. There is an exception at 7 kHz, but examining the beamforming plots (not shown) shows an acoustic source in the area of the model at this frequency, so the foam would not be expected to attenuate it strongly. (The 0° curve instead of the 80° curve in Fig. 6 should apply.) The reason that the noise actually increased by about 9 dB at that frequency with the introduction of the foam is not clear; the model may have been changed. Students were working on it during the test. The foam benefit below about 200 Hz is probably due to the reduction of the effect of the turbulent boundary layer by moving it off of the array.

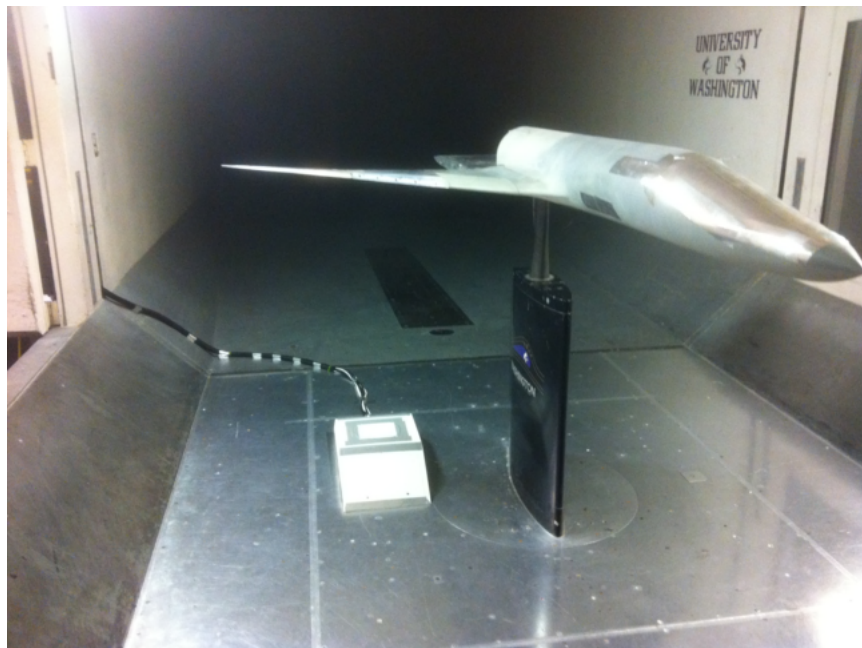


Fig.12. Setup for test in the Kirsten Wind Tunnel.

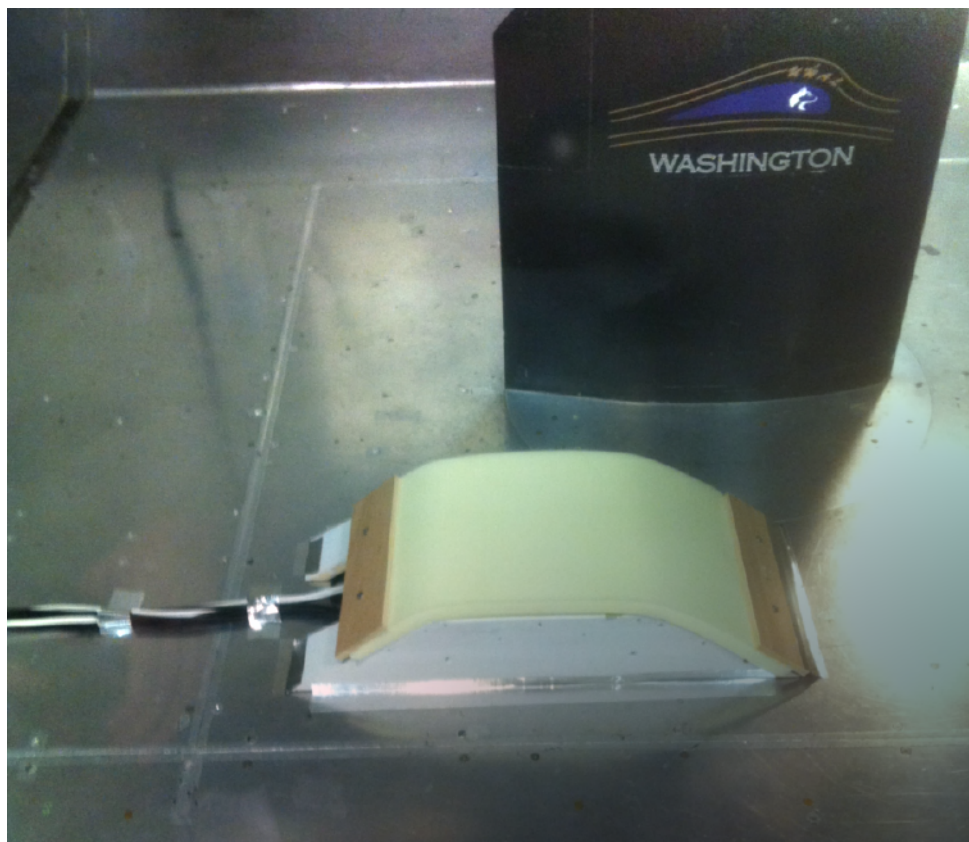


Fig.12. Foam installed on the array in the wind tunnel. Note: the foam fluttered at 50 m/s, necessitating a lower speed of 40 m/s for the test.

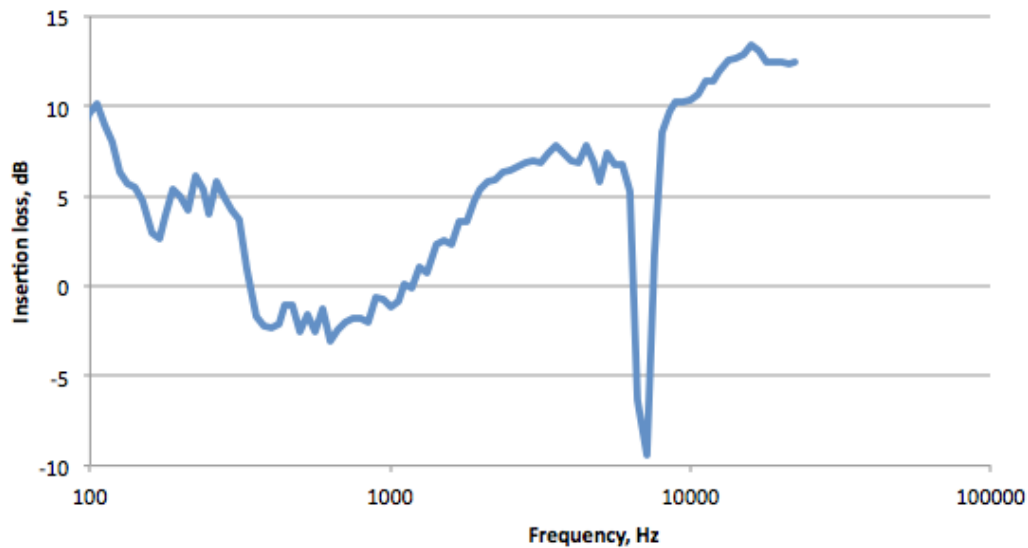


Fig.13. Reduction in the average of the off-diagonal array CSM elements due to installing foam on the array in the wind tunnel test.

4 CONCLUSIONS

Polyurethane foam over a phased array is promising for reducing wind tunnel background noise relative to model noise at frequencies above about 2 kHz. The samples of memory foam tested were more effective than conventional foam in the sense of providing better angular selectivity. A model based on the Delany and Bazley formula for the acoustic characteristics of porous media was not able predict the special performance of the memory foam, although it was somewhat successful for the other samples. Future work should should address improving the model to include more of the physics of memory foam, exercising the model to be sure that the apparent superiority of the memory foam sample is not just happenstance of its ordinary properties, as opposed to a special feature of memory foam, and exploring temperature effects and mounting techniques.

5 ACKNOWLEDGEMENT

The author is grateful to the Jack Ross and his crew at the University of Washington Aeronautical Laboratory for facilitating the wind tunnel test.

REFERENCES

- [1] Ehrenfried, K., L. Koop, A. Henning and K. Kaepernick, "Effects of wind-tunnel noise on array measurements in closed test sections," BeBeC Paper No. 2006-07, 2007.
- [2] Blacodan, D. "Spectral estimation method for noisy data using a noise reference," BeBeC Paper No. 2010-07, 2010.
- [3] Dougherty, R. P., "Beamforming in acoustic testing." Chapter 2 in *Aeroacoustic Testing*, T.J. Mueller, ed., Springer-Verlag, 2002.
- [4] Jaeger, S.M, W.C. Horne, and C.S. Allen, "Effect of surface treatment on array microphone self-noise," AIAA Paper AIAA-2000-1937, Lahaina, HI, June 12-14, 2000.

- [5] Remillieux, M., E.D. Crede, H.E. Camargo, R.A. Burdisso, W.J. Devenport, M. Rasnick, P. van Seeters, and A. Chou., "Calibration and demonstration of the new Virginia Tech anechoic wind tunnel," AIAA 2008-2911, 2008.
- [6] Sijtsma, P. and H. Holthusen, "Source location by phased array measurements in closed wind tunnel test sections," AIAA Paper No. 99-1814, 1999.
- [7] Allard, J.F. and N. Atalla, *Propagation of Sound in Porous Media - Modelling Sound Absorbing Materials*, Wiley, Chichester, West Sussex, United Kingdom, 2009.
- [8] Kidner, M.R.F. and C.H. Hansen, "A comparison and review of theories of the acoustics of porous materials," *International Journal of Acoustics and Vibration*, Vol. 13, No. 3, 2008. pp. 112-119.
- [9] Kino, N., G. Nakano, and Y. Suzuki, " Non-acoustical and acoustical properties of reticulated and partially reticulated polyurethane foams, " *Applied Acoustics* 73 (2012) 95–108.
- [10] Delany, M.E. and E.N. Bazley, "Acoustical properties of fibrous absorbent materials," *Applied Acoustics* 3 (1970) 105–116.
- [11] Bies, D.A. and C.H. Hansen, "Flow resistance information for acoustical design," *Applied Acoustics* 13 (1980) 357-391.
- [12] Dunn, I.P. and W.A. Davern, "Calculation of acoustic impedance of multi-layer absorbers," *Applied Acoustics* 19 (1986) 321–334.